Effect of Sample Size on the Microwave Heating Rate: Oil vs. Water

S. A. Barringer, E. A. Davis, and J. Gordon
Dept. of Food Science and Nutrition

K. G. Ayappa and H. T. Davis
Dept. of Chemical Engineering and Materials Science
University of Minnesota, Minneapolis, MN 55455

It is generally believed that oil samples heat faster in a microwave oven than do water samples of the same mass. For sufficiently large and thick samples this conventional wisdom is indeed correct, but this trend can be far from true in smaller samples. In a commercially-made home microwave oven, we observed that with decreasing sample size the heating rate of a water sample increases much faster than that of an oil sample. At 50 g the heating rate of a water sample is several times greater than that of an oil sample. Additionally, in studies of cylindrical samples in a customized oven having a unidirectional microwave source, the heating rate of water samples smaller than 2.4 cm in radius is greater than that of oil samples and is a strongly oscillatory increasing function of decreasing sample radius. Combining Maxwell's theory of microwave penetration and the heat conduction equation, we show that this previously unreported oscillatory heating behavior results from the added power absorbed by samples due to resonant absorption of microwaves. The added power arises from standing waves produced by internally reflected microwaves. This effect is small for oil because only 3% of the microwave power is reflected at an oil-air interface. On the other hand, 64% is reflected at a water-air interface, which causes strong resonant heating. Our findings might prove to be useful for future consumer food product development or oven design.

Introduction

The microwave oven has found many uses in the food and chemical engineering industries. The penetration of microwaves into a sample with the consequent volumetric heating makes microwaves an attractive thermal source for certain heating and cooking applications. Microwaves have found applications in tempering, drying, blanching, baking and reheating of products. The consumer microwave oven can be found in more than 90% of homes. Despite its popularity, however, the relationship between heating and sample characteristics remains poorly understood.

It is taken as conventional wisdom that a sample of oil will heat faster than the same-size sample of water. This is assumed to be due to the lower specific heat of oil, though it has also been noted that the internal electric field changes with dielectric properties, and therefore the sample power absorption may be different for oil and water (Prosetya and Datta, 1991). The causes of these different heating rates have not been analyzed in detail. Experiments have been compared for large samples with the assumption that the behavior observed would not change for small samples. One of the purposes of this work is to explore the validity of this assumption of invariance in size.

As samples increase in size, their total power absorption is known to asymptotically approach the power level of the oven (Sasaki et al., 1988; Mudgett, 1986). Thus, for large samples, the total power absorption is nearly size-independent. Theoretically, for smaller samples in the form of slabs the total power absorption shows strong oscillations with size (Fu and Metaxas, 1992). This oscillatory power absorption for thin slabs is the key to a number of patents (Peschek et al., 1992). This oscillatory power absorption should also affect the heating rate in small cylinders.

Table 1. Values of Dielectric Properties Used

	Water	Oil
Specific heat, C_p, $J \cdot kg^{-1} \cdot K^{-1}$	4,190	2,000
Thermal conductivity, k, $W \cdot m^{-1} \cdot K^{-1}$	0.609	0.168
Density, ρ, $kg \cdot m^{-3}$	1,000	900
Penetration depth, D_p, cm	3.6	36.8
Fraction power transmitted	0.36	0.97
Wavelength in sample, λ_s, cm	1.37	8.64
Dielectric constant, κ'	79.5	2.0
Dielectric loss, κ''	9.6	0.15

Heat-transfer coefficient, $h = 6 W \cdot m^{-2} \cdot K^{-1}$

In this work we systematically compare microwave heating of both large and small cylindrical samples of oil and water. We observe heating trends at the smaller radii that are unexpected and have not been previously reported. Maxwell's equation for electromagnetic wave propagation and the transient heat equation are used to predict the trends and to understand the relative importance of size and of the physical and dielectric properties in determining the heating rate of a sample.

Experimental Methods

Two types of microwave ovens were used in this study. Both ovens operate at 2,450 MHz. To exemplify the conventional or multidirectional power source, an ordinary household oven (Litton Model-1285) was chosen. The second oven used was a custom oven designed by Hung (1980) and modified with a horn antenna at the microwave entry port. In this oven the power is incident on the sample from one direction and terminates in a 5-gal (19-L) water load. The water load absorbs most of the transmitted and stray microwave power, minimizing back reflections. The purpose of the household oven is to demonstrate what occurs in the consumer's home microwave oven, and the purpose of the customized oven is to impose experimental conditions for which theory is more practicable.

The dielectric properties were measured using a Hewlett-Packard model 85070A dielectric probe. The specific heat, thermal conductivity, and heat-transfer coefficient were taken from literature for similar materials (Earle, 1973.) The density was determined by weighing the sample and measuring the volume of the weighed sample. The values used for this article are listed in Table 1.

Distilled water and Mazola corn oil were chosen for the study because they are common ingredients of food systems and their dielectric properties are very different. In all cases, the samples were refrigerated to 277 K before the experiment. They were then heated in the microwave oven to an approximate end temperature of 323 K. The time required to reach this end temperature was determined for each condition. At the end of heating, the samples were stirred for 30 s to determine the average final temperature, from which the average heating rate was determined. Samples were tested in triplicate and averages and standard deviations were calculated.

The heating rate was tested to determine if it is constant in this temperature range. A sample was heated for 20 s and then stirred to determine its average temperature at that time. The power was turned on for another 20 s and the new average temperature was determined. This was continued until the end of the run. By plotting these temperatures vs. time the samples were found to have a linear heating rate. This was true for both oil and water in the temperature range of 277 to 323 K. Further samples were heated without power interruption, and only initial and final average temperatures were determined.

The experimental conditions were somewhat different for the two microwave ovens. In the household oven, samples were placed in Pyrex beakers and exposed to multidirectionally impinging microwave radiation. The sample sizes were based on mass: 20, 30, 50, 100, 200, 300, 400, 500, 600, 700, 800, 900 and 1,000 g. The oven was rated at 600 W, and the samples were placed in the middle of the oven to assure that power was incident from all directions.

In the customized oven, samples were prepared so that their heat-transfer characteristics were approximately those of an infinite cylinder: we used in the sample design the engineering rule of thumb that to approximate infinite cylinder heat transfer the height to diameter ratio must exceed 3:1. In particular, samples were placed in graduated cylinders, and in all cases the height to diameter ratio exceeded 3:1. This ratio was not maintained for the household oven. Sample radii used were: 0.21, 0.30, 0.43, 0.49, 0.56, 0.58, 0.60, 0.73, 0.77, 0.80, 0.87, 0.95, 1.00, 1.11, 1.21, 1.35, 1.42, 1.80, 2.40, 3.04 and 3.90 cm. The oven was adjusted to 2,000 W, and the samples were always placed in exactly the same location in the oven for unidirectional microwave heating.

Theory

The model used assumes plane electromagnetic waves incident on an infinite cylinder of radius R as in the customized oven experiment. The incident power was assumed to be 45,000 $W \cdot m^{-2}$ to approximate the incident power in the custom oven. The values for the physical properties (specific heat, density, thermal conductivity, dielectric constant, and dielectric loss) were changed individually to determine their effect on the final sample power and temperature profiles.

Heat Transfer

For a well mixed sample of volume V and surface area A with volumetric power absorption $\overline{P}$, the average temperature, $\overline{T}$, predicted by a lumped parameter analysis is:

$$\overline{T} = \frac{\overline{P}V}{hA}[1 - e^{-\tau}] - (T_\infty - T_0)e^{-\tau} + T_\infty, \tag{1}$$

where

$$\tau = \frac{thA}{\rho V C_p}.$$

In Eq. 1, t is time, h is the heat-transfer coefficient, ρ is the material density, and C_p is the specific heat capacity. T_∞ is the ambient temperature and T_0 is the initial temperature of the liquid. The heat-transfer coefficient accounts for the heat transfer between the sample and its surroundings. All samples were at 277 K at the onset of heating. For small values of τ, Eq. 1 can be linearized and the expression for the heating rate is:

$$\frac{d\overline{T}}{dt} = \left[\frac{\overline{P}}{\rho C_p} + \frac{(T_\infty - T_0)hA}{\rho V C_p}\right]. \tag{2}$$

If convective heat transfer between the sample and the surrounding air is negligible, the heating rate simplifies to

$$\frac{d\bar{T}}{dt}=\frac{\bar{P}}{\rho C_p}. \tag{3}$$

The spatially averaged volumetric power absorbed in an infinite cylinder of radius R is:

$$\bar{P}=\frac{1}{\pi R^2}\int_{r=0}^{R}\int_{\phi=0}^{2\pi}P(r,\phi)r\,dr\,d\phi. \tag{4}$$

where P, the spatially varying volumetric power absorbed is predicted by solving Maxwell's equations. The material dielectric properties are assumed to be temperature-independent, and so the average power absorbed is assumed to be constant during heating.

Electromagnetic field and microwave power

For a uniform plane wave, with an electric field of intensity E_0, oriented along the long axis of the cylinder (TM^z polarization) the electric field distribution in the cylinder obtained by solving Maxwell's equations with a time dependence of the form $e^{-i\omega t}$ (Ayappa et al., 1992) is:

$$E_z(r,\phi)=\sum_{n=0}^{n=\infty}c_nJ_n(kr)\cos n\phi. \tag{5}$$

where the coefficients

$$c_n=E_0\epsilon_n i^n\left[\frac{J_n'(Rk_0)H_n^{(1)}(Rk_0)-J_n(Rk_0)H_n^{(1)\prime}(Rk_0)}{\sqrt{\kappa^*}J_n'(Rk)H_n^{(1)}(Rk_0)-J_n(Rk)H_n^{(1)\prime}(Rk_0)}\right] \tag{6}$$

and

$$\epsilon_n=\begin{cases}1 & n=0;\\ 2 & \text{otherwise.}\end{cases}$$

$\kappa^*=\kappa'+i\kappa''$ is the complex permittivity where κ' is the dielectric constant and κ'' is the dielectric loss of the medium. In Eq. 6, the propagation constants in free space, k_0, and in the sample, k, are:

$$k_0=(2\pi/\lambda_0) \tag{7}$$

and

$$k=(2\pi/\lambda_0)\sqrt{\kappa'+i\kappa''}. \tag{8}$$

$H_n^{(1)}$ is the Hankel function of the first kind and J_n is the nth—order Bessel function of the first kind (Abramowitz and Stegun, 1970). In the above equations, $i=\sqrt{-1}$ and the magnetic permeability of the sample is assumed to be that of free space.

With a knowledge of the electric field distribution in the sample, the absorbed microwave power is:

$$P(r,\phi)=\frac{1}{2}\omega\epsilon_0\kappa''E_zE_z^*, \tag{9}$$

where ϵ_0 is the free space dielectric constant and $\omega=2\pi f$, where f is the frequency of radiation. In Eq. 9, E_z^* is the complex conjugate of E_z. The microwave power deduced from Eq. 9 is used to predict the average microwave power absorbed.

The dielectric constant and loss determine the wavelength within a sample, penetration depth, and reflection coefficient. At 2,450 MHz the wavelength in freespace (λ_0) is 12.24 cm. The wavelength within the sample (λ_s) is 8.64 cm for oil and 1.37 cm for water. The formula for λ_s is:

$$\lambda_s=\frac{\lambda_0}{\sqrt{\frac{\kappa'}{2}}\sqrt{\sqrt{1+\left(\frac{\kappa''}{\kappa'}\right)^2}+1}} \tag{10}$$

The penetration depth, D_p, or distance at which the incident electric field has decayed to $1/e$ of its incident level is:

$$D_p=\frac{\lambda_0}{\pi\sqrt{2\kappa'}\sqrt{\sqrt{1+\left(\frac{\kappa''}{\kappa'}\right)^2}-1}}. \tag{11}$$

As the dielectric constant and loss vary, the penetration depth changes and the electric field in the sample is altered. For oil, the penetration depth is 36.8 cm or much greater than common sample sizes. For water, the penetration depth is 3.6 cm which is in the range of many samples. When the sample is much larger than the penetration depth, the electric field and therefore power absorption are the greatest at the incident face, and decay exponentially into the sample. All of the transmitted power is absorbed. When the sample width is a few penetration depths or less, significant amounts of the electric field reach the back face of the sample to be reflected or lost.

To understand qualitatively what is occurring in the cylinder, we can look at the reflection and transmission that occur at the interface of air with a semiinfinite slab of the material. The Poynting vector or the power flux associated with a propagating electromagnetic wave is:

$$S=\frac{1}{2}Re[E\times H^*], \tag{12}$$

where *Re* denotes the real part of the quantity within brackets. It follows from Eq. 12 that, for a uniform plane wave propagating in medium 1, incident on a semiinfinite slab (medium 2) located at the origin, the incident power is:

$$S_{\text{in}}=\frac{E_0^2\alpha_1}{\mu_0\omega}, \tag{13}$$

and the transmitted power is:

$$S_{\text{tr}}=\frac{E_0^2T_{1,2}^2\alpha_2}{\mu_0\omega}. \tag{14}$$

In Eqs. 13 and 14, α the phase factor is related to the wavelength of radiation, λ_s, in the medium:

$$\alpha_i = \frac{2\pi}{\lambda_s^{(i)}} \quad \text{where} \quad i = 1,2 \tag{15}$$

and $T_{1,2}$, the transmission coefficient is expressed as:

$$T_{1,2} = \sqrt{\frac{4(\alpha_1^2 + \beta_1^2)}{(\alpha_1 + \alpha_2)^2 + (\beta_1 + \beta_2)^2}}, \tag{16}$$

where the attenuation factor β is related to the penetration depth D_p:

$$\beta_i = \frac{1}{D_p^{(i)}} \quad \text{where} \quad i = 1,2. \tag{17}$$

Using the expressions for incident and transmitted powers, and replacing α by λ, we find that the fraction of the incident power transmitted at the interface is:

$$\frac{S_{tr}}{S_{in}} = T_{1,2}^2 \frac{\lambda_s^{(1)}}{\lambda_s^{(2)}}. \tag{18}$$

At the air to oil interface, 97% of the incident power is transmitted into the sample. The power that is not absorbed by the sample is lost from the back face of the sample where again 97% of the power is transmitted. Standing waves in the oil sample are therefore weak since only 3% of the field is reflected.

At the air to water interface, 36% of the incident power is transmitted into the sample. Thus, the power transmitted into the sample is lower than for oil, but since 64% of the power transmitted through the sample without being absorbed is again reflected off the back face, this creates the potential for standing wave patterns. The consequence is that in small samples the field strength within the sample is increased many fold.

When reflections from the back face are present in either the slab or cylinder, constructive and destructive interference creates standing wave patterns that produce peaks and valleys of power absorption. Thus, the exact sample size is important when determining the power absorption and heating rate. We ignore the presence of the glass containers since there is little reflectance of microwaves at the air/glass interface and little power loss in the glass.

Results and Discussion

In the household oven, Figure 1, the heating rate of both oil and water is shown to be size-dependent. For the larger samples ranging from 300 to 1,000 g, both oil and water show similar trends. In this range, the average heating rate increases slightly as sample size decreases. The larger the sample, the lower the average heating rate. At these dimensions, however, oil samples heat approximately twice as fast as water.

In the case of the smaller samples ranging from 20 to 300 g, the oil and water average heating trends are contrary to conventional wisdom. As the samples decrease in size, the average heating rate of oil increases slightly and then peaks or levels off. However, the average heating rate of water increases

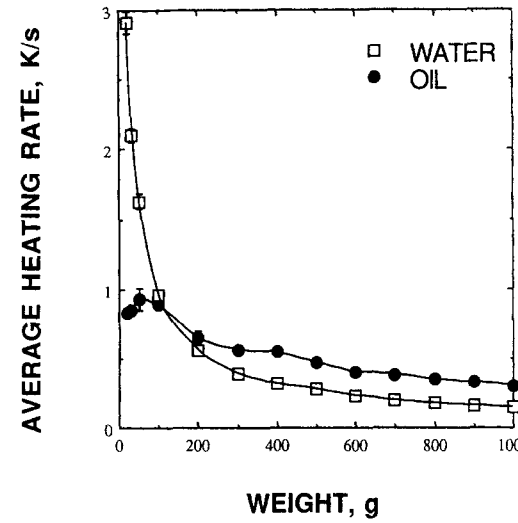

Figure 1. Measured average heating rates of oil and water as a function of sample weight in a household microwave oven.

At large samples sizes, oil heats approximately twice as fast as water, and heating is dominated by the lower heat capacity of oil over water. However, as sample size decreases the heating rates of water become considerably greater than those of oil.

dramatically, to more than ten times. This is counterintuitive, as the heating rates would be expected to be nearly constant at these sample sizes. Also surprising is that at 100 g the average heating rate of water surpasses that of oil. For samples smaller than 100 g, water heats faster than oil. This result has not been previously reported.

Figure 2 illustrates a similar size dependence with a customized oven. Average heating rates of the large samples ranging

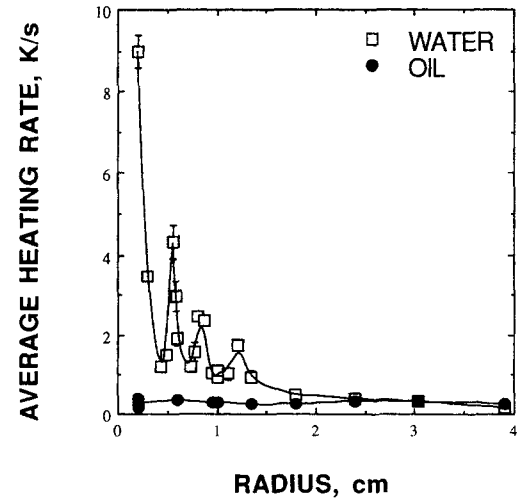

Figure 2. Measured average heating rates of oil and water as a function of sample radius in a customized microwave oven with a unidirectional source.

Similar trends with sample size are observed here as in the home oven (Figure 1). When resonance occurs at a particular sample size, a local maximum in heating rate is observed. The intensity of the maximum decreases as the sample radii get larger. The resonances are strong for the water samples and much weaker in the case of oil. These resonant heating conditions were not observed in the home oven.

from 2 to 4 cm in radii increase slightly as the samples decrease in size. Both oil and water heat at approximately the same rate in this range, with oil heating faster than water at the largest sample size. For the smaller samples (0.2 to 2.0 cm radii), the average heating rate of oil is approximately constant with decreasing sample size. The average heating rate of water again increases dramatically. However, in this oven the increase is not a smooth curve but is strongly oscillatory with three peaks, at 1.21, 0.80 and 0.56 cm.

The theoretical average heating rate vs. radius, predicted with Eq. 2, is shown in Figure 3. For the range of sample sizes used in the custom oven experiments, convective heat losses to the ambient air are small, and the difference in average heating rates predicted by Eq. 2 and Eq. 3 was negligible. Convective heat losses were found to be important for smaller samples well below the radii used in the experiments. The theoretical heating rates predict the trend in Figure 2, the case for which theory and experimental setup are comparable. The average heating rates of large samples with radii ranging from 2 to 4 cm increase slightly as the samples decrease in size, with oil heating faster than water at samples larger than 2.4 cm. The smaller samples in the 0.1 to 2.0 cm range show oil heating at a nearly constant rate as the samples decrease in size, while the average heating rate of water increases dramatically and is strongly oscillatory. There are peaks and valleys throughout the entire range for both oil and water, though oscillations in the case of oil are very weak. As the samples decrease in size, the peaks become larger.

The factors that determine the sample heating rate are the power absorption and its conversion to energy. In this study, the effects of thermal conductivity are not important since only average heating rates are examined and the heat lost to the environment is very small. The power absorption is determined by the dielectric properties and sample size. Therefore, the factors that could be important in explaining the heating trends of oil vs. water are the specific heat, density, sample size, and complex dielectric constant.

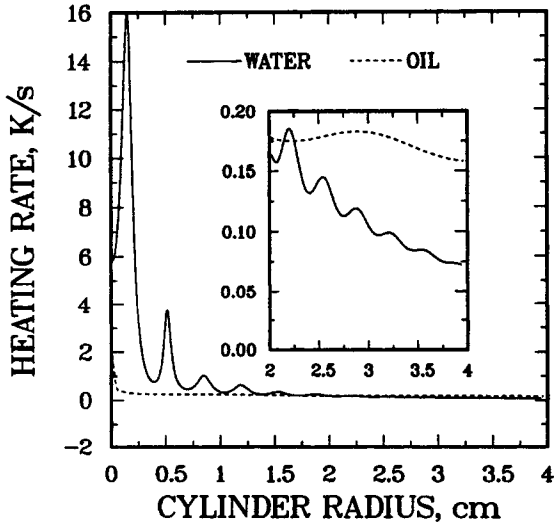

Figure 3. Predicted average heating rates in cylindrical samples exposed to plane waves with the electric field oriented along the axis of the cylinder.

Heating rates predict the experimentally observed resonant heating at similar sample radii for the water samples.

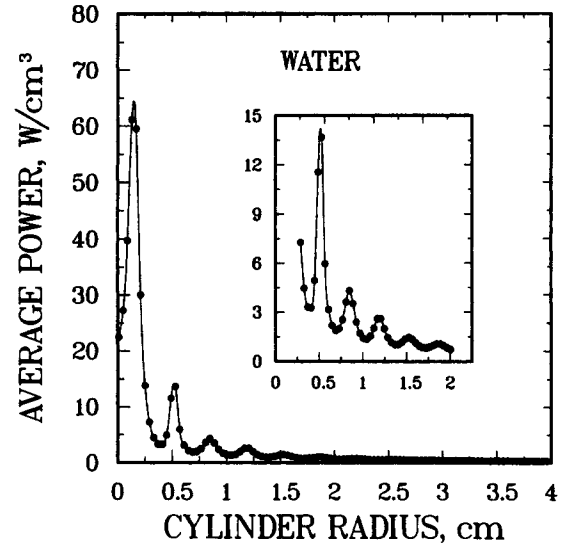

Figure 4. Average power absorbed in cylindrical samples of water as a function of sample radii.

The electric field is oriented along the long axis of the cylinder. The peaks in the power absorption indicate a resonant condition. Maxima in average heating rates of water were observed at similar radii as in the oven experiment (Figure 2).

In the case of large samples, the heating trends are determined primarily by the specific heat. The theoretical average power absorption for oil and water samples with radii greater than 3 cm is nearly the same, as shown in Figure 5. The density is very similar for the two samples; 900 $kg \cdot cm^{-3}$ for oil and 1,000 $kg \cdot cm^{-3}$ for water. If the density of oil is changed to 1,000 $kg \cdot cm^{-3}$ with no other changes in physical properties, the theoretical heating rate for the 3-cm sample is only changed from 0.151 to 0.137 K/min. This is a small effect. The specific heat of oil is 2,100 $J \cdot kg^{-1} \cdot K^{-1}$, as compared to 4,190 $J \cdot kg^{-1} \cdot K^{-1}$

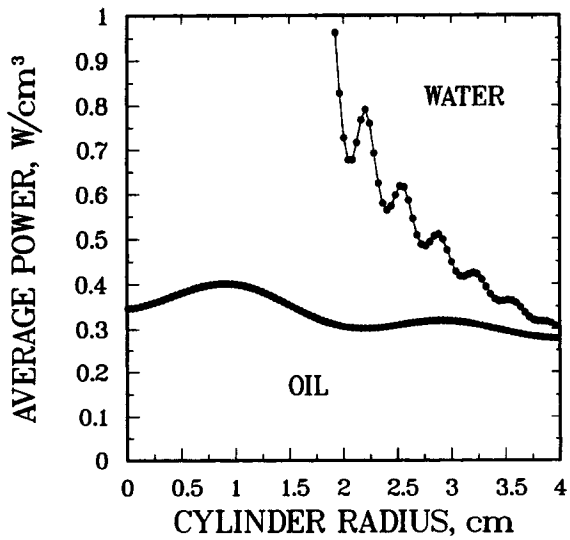

Figure 5. Average power absorbed in cylindrical samples of oil as a function of sample radii.

The strong resonant power absorption conditions present for water are absent, and the power absorbed is a weak function of radius. The power absorption for water in the same range is shown for comparison. At large sample sizes, the power absorption for both water and oil are comparable and heating rates are dominated by the difference in heat capacities as shown in Figures 1 and 2.

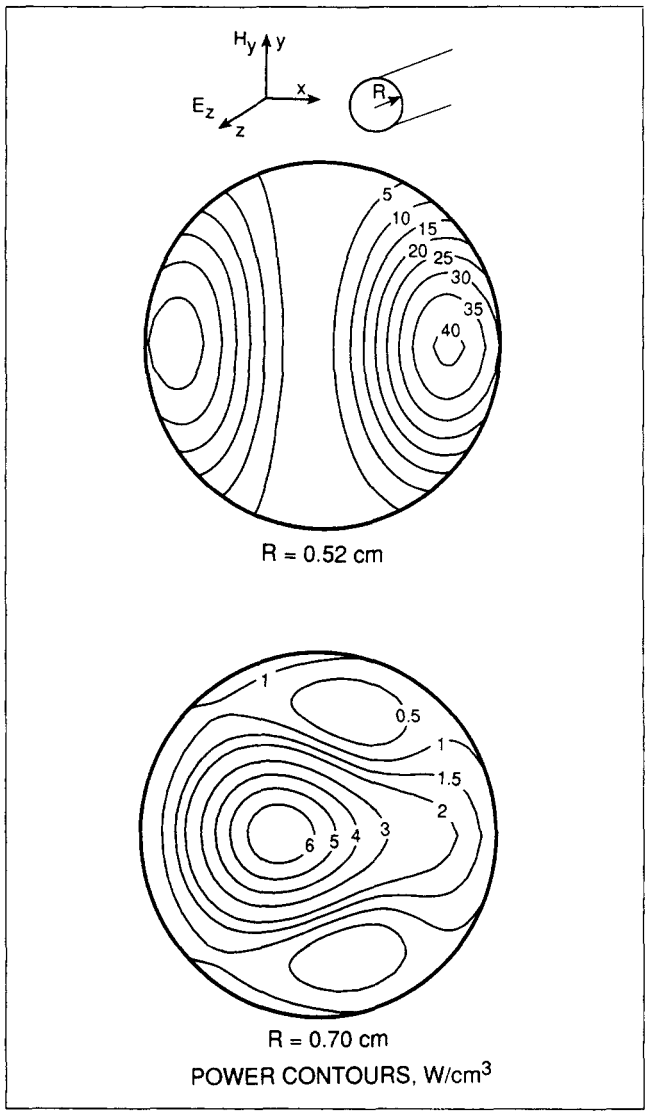

Figure 6. Internal power contours for cylinders of water with radii 0.52 and 0.70 cm.

A radius of 0.52 cm corresponds to the second resonance peak in Figure 4 where the average power absorbed is 15.26 W/cm^2. A radius of 0.70 cm corresponds to a nonresonant condition and the average power absorbed is only 1.88 W/cm^2.

for water. Given identical power absorption, theoretically the oil samples heat twice as fast as the water, which in fact accounts for the differences seen experimentally.

For smaller samples, the heating rate can no longer be explained by thermal properties alone. The density has little effect and the specific heat, while still affecting heating rate, cannot explain water heating faster than oil. The power absorption, determined by the dielectric properties, must be much higher for small samples of water. This is shown to be true in Figures 4 and 5.

This difference in the power absorption of oil vs. water is determined by the sample dielectric properties. For oil, $\kappa^* = 2.0 + i0.15$, giving a penetration depth of 36.8 cm. This means a large percentage of the power is not absorbed in the samples. Of the field that reaches the back face, only 3% is reflected. This creates weak standing waves. The resonance is slight, resulting in small peaks of power absorption. With decreasing sample size, only a slight increase in total power absorbed and a very small increase in heating rate is observed.

For water, $\kappa^* = 79.5 + i9.6$, giving a penetration depth of 3.6 cm. This falls in the middle of the experimental range. The smaller samples have a large amount of the field reaching the back face, while the large samples absorb most of the available power. For the small samples, a large percentage of the power reaches the back face. At this point, 64% of the field is reflected back into the sample, creating strong standing waves.

The power from the front and back faces of the sample can combine constructively or destructively. The exact radius of the sample will determine the phase of the returning wave and the degree of constructive and destructive interference. Figure 6 shows the power distribution in the sample at two different radii. At a radius of 0.52 cm, the waves interfere constructively giving rise to strong resonance and an average power absorption of 15.26 W·cm^{-3}. At 0.7 cm, the sample is no longer at a resonant condition and the average power absorbed is only 1.88 W·cm^{-3}. This interference explains the peaks and valleys of power absorption in Figures 4 and 5, which is seen again in the theoretical average heating rates of Figure 3. The theoretically predicted peaks in heating rates are at the same radii as the experimental heating rates in Figure 2.

Conclusion

For sufficiently large samples, the relative microwave heating rates of oil and of water samples of the same weight are determined primarily by the ratio of their heat capacities. The dielectric properties of these substances change the internal electric field profile, but the total power absorbed is quite similar.

With decreasing sample sizes, the dielectric properties begin to dominate the microwave heating. The weak internal reflections of oil result in an almost size-independent power absorption and therefore result in a nearly uniform temperature distribution throughout the sample. Strong resonances (standing waves) in water create an oscillatory total power absorption that gives large peaks in the heating rate at certain radii.

The experimental trends of small samples in the custom oven are completely accounted for by theory based on the assumption of constant properties. The custom oven experiments demonstrate that in a highly controlled microwave setup the sample size-dependent heating fluctuations can be an important factor. In the household oven, the most common microwave situation, the multidirectionality of the microwave field weakens the effect, but still a strong size-dependent heating rate is observed for small sample sizes.

Notation

C_p = specific heat capacity, J·kg^{-1}·K^{-1}
D_p = penetration depth, m^{-1}
E = electric field intensity, V·m^{-1}
f = frequency of incident radiation, Hz
h = heat-transfer coefficient, W·m^{-2}·K^{-1}
H = magnetic field intensity, Amp·m^{-1}
J = current flux, Amp·m^{-2}
k = thermal conductivity, W·m^{-1}·K^{-1}
k = propagation constant, m^{-1}
k_0 = free space propagation constant, m^{-1}
P = volumetric power absorbed, W·m^{-3}
$\bar{P}$ = spatially averaged volumetric power absorbed, W·m^{-3}
R = radius of sample, m

S = power flux or Poynting vector, $W \cdot m^{-2}$
S_{in} = incident power flux, $W \cdot m^{-2}$
S_{tr} = transmitted power flux, $W \cdot m^{-2}$
t = time, s
T = temperature, K
$T_{1,2}$ = transmission coefficient
$\overline{T}$ = spatially averaged temperature, K

Greek letters

α = phase constant, m^{-1}
β = attenuation constant, m^{-1}
κ' = relative dielectric constant
κ'' = relative dielectric loss
κ^* = complex relative permittivity
λ_0 = free-space wavelength, m
λ_s = wavelength in sample, m
μ_0 = free space permeability, $He \cdot m^{-1}$
ρ = density, $kg \cdot m^{-3}$
ω = angular frequency, $Rad \cdot s^{-1}$

Subscripts

0 = free space
1 = medium 1
2 = medium 2
in = incident
tr = transmitted

Superscripts

(1) = medium 1
(2) = medium 2
* = complex conjugate

Literature Cited

Abramowitz, M., and I. A. Stegun, *Handbook of Mathematical Functions*, 9th ed., Dover, New York (1970).

Ayappa, K. G., H. T. Davis, E. A. Davis, and J. Gordon, "Two-Dimensional Finite Element Analysis of Microwave Heating," *AIChE J.*, **38**, 1577 (1992).

Earle, R. L., *Unit Operations in Food Processing*, Pergamon Press, New York (1973).

Fu, W., and A. Metaxas, "A Mathematical Derivation of Power Penetration Depth for Thin Lossy Materials," *J. Microwave Power*, **27**, 217 (1992).

Hung, C. C., "Water Migration Structural Transformation of Oven Cooked Meat," PhD Dis., Univ. of Minnesota, Minneapolis (1980).

Mudgett, R. E., "Electrical Properties of Foods," *Engineering Properties of Foods*, M. A. Rao and S. S. H. Rizvi, eds., Marcel Dekker, New York (1986).

Peschek, P., W. H. Atwell, M. Krawjecki, and G. Anderson, U. S. Patent No. 5140121 (1992).

Prosetya, H., and A. K. Datta, "Batch Microwave Heating of Liquids: An Experimental Study," *J. Microwave Power*, **26**, 215 (1991).

Sasaki, K., A. Shimada, K. Hatae, and A. Shimada, "Influence of the State of Mixing of the Sample on Total Absorbed Energy in Microwave Cooking," *Agric. Biol. Chem.*, **52**, 2273 (1988).

Manuscript received June 9, 1993, and revision received Oct. 6, 1993.